J Fluoresc (2011) 21:893–899
DOI 10.1007/s10895-010-0604-6

ORIGINAL PAPER

The Role of the Eu^{3+} Concentration on the $SrMoO_4$:Eu Phosphor Properties: Synthesis, Characterization and Photophysical Studies

Ana Paula A. Marques · Marcos Takashi S. Tanaka · Elson Longo · Edson R. Leite · Ieda Lucia Viana Rosa

Received: 29 October 2009 / Accepted: 29 January 2010 / Published online: 23 February 2010
© Springer Science+Business Media, LLC 2010

Abstract $SrMoO_4$ doped with rare earth are still scarce nowadays and have attracted great attention due to their applications as scintillating materials in electro-optical like solid-state lasers and optical fibers, for instance. In this work $Sr_{1-x}Eu_xMoO_4$ powders, where x=0.01; 0.03 and 0.05, were synthesized by Complex Polymerization (CP) Method. The structural and optical properties of the $SrMoO_4$:Eu^{3+} were analyzed by powder X-ray diffraction patterns, Fourier Transform Infra-Red (FTIR), Raman Spectroscopy, and through Photoluminescent Measurements (PL). Only a crystalline scheelite-type phase was obtained when the powders were heat-treated at 800 °C for 2 h, 2θ=27.8° (100% peak). The excitation spectra of the $SrMoO_4$:Eu^{3+} ($\lambda_{Em.}$=614 nm) presented the characteristic band of the Eu^{3+} $^5L_6$ transition at 394 nm and a broad band at around 288 nm ascribed to the charge-transfer from the O (2p) state to the Mo (4d) one in the $SrMoO_4$ matrix. The emission spectra of the $SrMoO_4$:Eu^{3+} powders ($\lambda_{Exc.}$=394 and 288 nm) show the group of sharp emission bands among 523–554 nm and 578–699 nm, assigned to the $^5D_1 \rightarrow {}^7F_{0,1 \text{and } 2}$ and $^5D_0 \rightarrow {}^7F_{0,1,2,3 \text{ and } 4}$, respectively. The band related to the $^5D_0 \rightarrow {}^7F_0$ transition indicates the presence of Eu^{3+} site without inversion center. This hypothesis is strengthened by the fact that the band referent to the $^5D_0 \rightarrow {}^7F_2$ transition is the most intense in the emission spectra.

Keywords Europium · Molybdate · Complex polymerization method · Photoluminescence

A. P. A. Marques · M. T. S. Tanaka · E. R. Leite · I. L. V. Rosa (✉)
Laboratório Interdisciplinar de Eletroquímica e Cerâmica, Centro Multidisciplinar de Desenvolvimento de Materiais Cerâmicos, Departamento de Química, Universidade Federal de São Carlos, C. Postal 676, 13565-905 São Carlos, SP, Brazil
e-mail: ilvrosa@ufscar.br

E. Longo
CMDMC, LIEC, Instituto de Química, Universidade Estadual Paulista, 14801-907 Araraquara, SP, Brazil

Introduction

Alkaline earth molybdates, $M_{1-x}TR_xMoO_4$ (M=Ca, Sr, Ba; TR=Eu, Tb, Tm), presenting a distorted tetragonal scheelite-like (β) structure have characteristic properties and are receiving great interest because of their potential application in areas such as laser hosts, phosphors, optical fibers, pigments, humidity sensors, magnetic materials, ionic conductors, catalysts, etc [1, 2]. Besides, molybdates are being considered good hosts for luminescent materials due to its excellent thermal and chemical stability [3, 4].

Powders and films of molybdates with a scheelite-like crystalline structure have been synthesized through different methodologies [5–9]. Some of these procedures, however, promote the obtention of inorganic materials with relatively large particle sizes, where several of them could present little homogeneity in their morphology and composition [10].

The Complex Polymerization (CP) Method allows the use of relatively low annealed temperatures and reduces the segregation of the metal, promoting the homogeneity in the composition of the material in molecular scale. These advantages permit a bigger distribution of cations, promoting the chemical uniformity through all polymeric material, favoring the homogeneity of the multicomponent oxides [11, 12]. Because of these characteristics the CP Method will be used in this work to prepare doped $SrMoO_4$ with Eu^{3+} in different concentrations of this ion in its matrix.

Europium in its trivalent state is one of the most studied through the luminescence spectroscopy among the rare earth elements as a consequence of the simplicity of its spectra and due to the wide application as red phosphor in color TV screens. This ion have also attracted significant attention of the researchers due to their potential application as biological sensors, phosphors, electroluminescent devices, optical amplifiers or lasers when it is used as doping in a variety of materials [13, 14]. These advantages are mainly originated to the fact that the Eu^{3+} ^5D_J (J=0, 1, 2 and 3) excited states are well separated from the ground terms $^5F_{J'}$ (J′=0, 1, 2, 3, 4, 5 and 6). The main emitting excited level, $^5D_0$, and the ground state one, $^7F_0$, are not splited, giving rise to only one peak related to the $^5D_0 \rightarrow {}^7F_0$ transition (when the Eu^{3+} ion is located in identical sites having C_s, C_n or C_{nv} symmetries), making easy the interpretation of the spectral, providing information on the eventual existence of different Eu^{3+} sites. The $^5D_0 \rightarrow {}^7F_1$ transition usually is given as reference since it is allowed by forced magnetic dipole mechanism, and consequently its intensity is not considerably modified by disturbance of the crystalline field around the Eu^{3+} ion. Additionally Eu^{3+} $^5D \rightarrow {}^7F$ transitions present long lifetime (milliseconds) and great Stokes displacement when the photoluminescent spectrum is gotten by direct excitation of the $^5L_6$ level (~394 nm) or through another excited state [15].

There are small amount of research on the optical properties of $SrMoO_4$ doped rare earth. Recently, Ho^{3+}:$SrMoO_4$ single crystal was grown by the Czochralski method in N_2 atmosphere and the polarized absorption spectra, emission spectra and the lifetime decay curves were measured at room temperature [7]. The same researchers [5] published the work where Er^{3+}:$SrMoO_4$ crystal of high optical quality was grown using this method and the room temperature polarized absorption and emission spectra together with the lifetime decay curve were measured. In another paper the authors described that single crystal of Tm^{3+}:$SrMoO_4$ was successfully prepared by the same methodology and grown along the (0 0 1) orientation in N_2 atmosphere. The refractive index of $SrMoO_4$ crystal was measured at room temperature. The radiative probabilities, radiative branching ratios, radiative lifetimes and stimulated emission cross sections of Tm^{3+} in $SrMoO_4$ were obtained [16]. A new Eu activated molybdate phosphor, $SrMoO_4$, was fabricated using solid-state method in order to prepare fluorescent material for white Light Emitting Diodes (LEDs) [17], and more recently rare-earth ions (Eu^{3+}, Tb^{3+}) doped $AMoO_4$ (A = Sr, Ba) particles with uniform morphologies were successfully prepared through a facile solvothermal process using ethyleneglycol (EG) as protecting agent [18]. According to our knowledgements, any paper deals with the Eu^{3+} photoluminescent properties in this matrix using the methodology employed in this study. The investigation on the synthesis and room temperature photoluminescent properties of the Eu^{3+} in different concentrations doping $SrMoO_4$ matrix prepared by the CP Method, as well as its characterization by X-ray diffraction patterns (XRD), Fourier Transform Infra-Red (FTIR) and Raman Spectroscopy are presented here for the first time.

Experimental

Materials

The chemical reagents used in this study without further purification were molybdenum trioxide MoO_3 (Synth 85%), $SrCO_3$, (Mallinckrodt 99%), europium (III) oxide (Aldrich, USA, 99.999%), citric acid ($H_3C_6H_5O_7$) (Mallinckrodt 99%) and ethylene glycol ($HOCH_2CH_2OH$) (J. T. Baker 99%).

Preparation of $Sr_{1-x}Eu_xMoO_4$ (SEMO) and pure $SrMoO_4$ (SMO) powders

$Sr_{1-x}Eu_xMoO_4$ (SEMO) powders (x=0.0; 0.01; 0.03 and 0.05), were produced by CP Method, the Fig. 1 is a flow chart representing the preparation of SEMO powders. In the synthesis of the SEMO powders the molar ratio between Sr^{+2} and Eu^{+3} was set in the respective proportions of 99:1, 97:3 and 95:5. The obtained dark-brown powders were pulverized using a mortar and were finally annealed at 800 °C for 2 h under ambient atmosphere, using a heating rate of 5 °C/min. The obtained white powders with its respective amount of Eu^{3+} ions were denoted as SEMO.

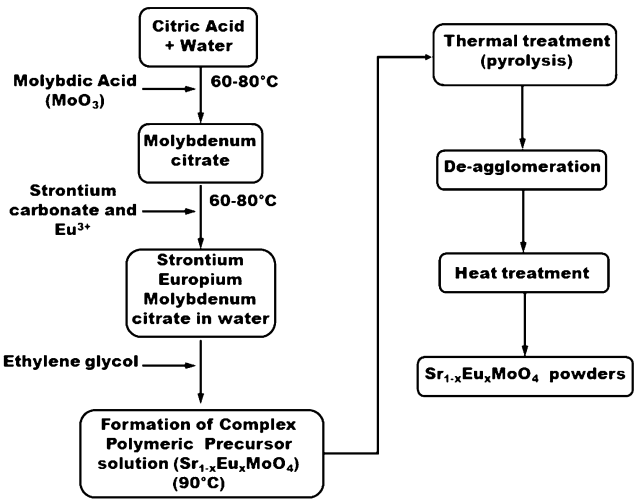

Fig. 1 Flow chart representing the procedure employed in the synthesis of SEMO powders

Characterizations

The structural evaluation and the unit cell volume of the SEMO and SMO powders were determined through its X-ray diffraction patterns (XRD) using a Rigaku Dmax2500PC diffractometer. The average crystallite diameter (Dcrys) of the materials after the heat treatment was determined using the (112) diffraction peak of the $SrMoO_4$ phase, which 2θ is located at around 26.5° [10]. Fourier transform infrared (FTIR) spectra were obtained in an Equinox/55 Bruker spectrometer, while Raman spectroscopy data were obtained in a RFS/100/S Bruker FT-Raman equipment. The room temperature photoluminescence (PL) data of the SEMO powders were obtained in a Jobin Yvon-Fluorolog spectrofluorometer using a 450 W xenon lamp as excitation energy source. Luminescence lifetime measurements were carried out as well using a 1934D model spectrophosphorometer coupled to the spectrofluorometer.

Results and discussion

Figure 2 presents the XRD patterns of the SEMO powders containing (a) 1.00, (b) 3.00, and (c) 5.00% of Eu^{3+} and SMO powders annealed at 800 °C for 2 h. According the JCPDS data base [19] all diffraction peaks were indexed as a scheelite-like single phase of the $SrMoO_4$ presenting the tetragonal symmetry. The lattice parameters **a** and **c** were calculated from the peak positions displayed in this figure, using the least square refinement from the REDE93 program. Table 1 presents the crystallite sizes and lattice constants **a** and **c** of tetragonal structure of $SrMoO_4$ and $SrMoO_4$:Eu^{3+} powders prepared by CP Method and heat

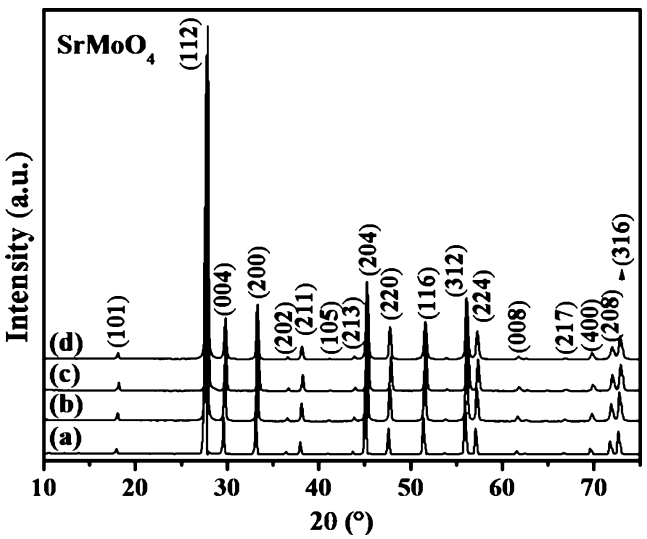

Fig. 2 XRD patterns for the SMO (a) and SEMO powders containing 1.00 (b), 3.00 (c) and 5.00% (d) of Eu^{3+} heat treated at 800 °C for 2 h

Table 1 Crystallite sizes and comparison of tetragonal lattice constants ***a*** and ***c*** of tetragonal structure of SMO and SEMO powders prepared by CP Method and heat treated at 800 °C for 2 h

Sample	Diameter crystallite[a] ($D_{crys.}$ nm)	Lattice constants (Å)	
		a	***c***
SMO	48±2.4	5.399(0)	12.041(1)
SEMO 1.00% Eu^{3+}	48±2.4	5.389(1)	12.018(2)
SEMO 3.00% Eu^{3+}	48±2.4	5.379(1)	11.100(3)
SEMO 5.00% Eu^{3+}	40±2.0	5.386(0)	12.002(2)

a=5.394 Å and ***c***=12.02 Å [17]

[a] Calculated using the (112), 100% diffraction peak

treated at 800 °C for 2 h. The values of **a** and **c** for the crystalline SMO and SEMO powders are also in accordance to reported data for bulk material, where **a**=5.3944 Å and **c**=12.020 Å [19].

The average crystallite diameters (D_{crys}) of the materials after the heat treatments were determined using the (112) diffraction peak of the $SrMoO_4$ phase, which 2θ is located at around 26.5° (100% peak) [10]. It is observed in this table that the SEMO samples containing 1.00 and 3.00% of Eu^{3+} presented the same crystallite size values of 48 nm, as well as the SMO powder heat treated at 800 °C. It is also noticed that when the Eu^{3+} concentration was 5.00% the material presented a decrease in this parameter, which value was evaluated as 40 nm. This decrease in the crystallite size values indicates the substitution of Sr^{2+} present in the $SrMoO_4$ lattice for Eu^{3+}. Since the Eu^{3+} ratio is a little small (0.109 nm) than Sr^{2+} ratio (0.132 nm), it is expected that the $[EuO_8]$ clusters linked to the $[MoO_4]^{2-}$ ionic tetragonal ones will result in small unit cell when compared to the $[SrO_8]$ clusters linked to the $[MoO_4]^{2-}$.

The scheelite primitive cell presents 26 different vibration modes: $\Gamma_{Td} = 3\ A_g + 5\ A_u + 5B_g + 3B_u + 5E_g + 5E_u$, but only ($A_g$, B_g and E_g) are Raman-active, while the odd modes ($4A_u$ and $4E_u$) can be registered only in the infrared spectra. The tree B_u vibrations are silent modes; one A_u and one E_u modes are acoustic vibrations. The spontaneous Raman spectra with the assignments of the Raman-active vibration modes of the pure SMO powders were already studied [10] and are compared with SEMO powders in this work. According to Basiev [20], the primitive cell of SMO includes two formula units, the $[MoO_4]^{2-}$ ionic group, with strong covalent Mo–O bonds, called internal modes, and the weak coupling between the $[MoO_4]^{2-}$ ionic group and the Sr^{2+} cations, the external modes. The internal vibrational ones correspond to the vibrations within the $[MoO_4]^{2-}$ group, with an immovable mass center. The external or lattice phonons correspond to the motion of the Sr^{2+} cations and the rigid molecular unit. The $[MoO_4]^{2-}$ tetrahedral ion in the free space presents T_d symmetry.

Spontaneous Raman spectra for SMO and SEMO heat treated at 800 °C are presented in Fig. 3 and detailed in Table 2. The Raman spectra showed the well-resolved sharp peaks for the SMO and SEMO powders treated at 800 °C, indicating that the synthesized powders were highly crystallized. It was possible to detect some differences in the Raman spectra of the SEMO samples doped with the specified Eu^{3+} concentrations and the SMO sample heat treated at the same temperature, theses differences are presented with (*) in the Fig. 3. These differences are assumed as referring to linked strong variations between Mo-O caused by the presence of europium in the structure.

The FTIR spectra of the SMO and SEMO powders are showed in Fig. 4, the measurements were carried out in the transmittance mode. In the present tetrahedral symmetry (T_d) only the $F_2(\nu_3, \nu_4)$ modes are IR active. The band at around 403 cm^{-1}, related to the $F_2(\nu_4)$ vibration mode, is observed in all the samples, SMO and SEMO. The spectra of the SMO and SEMO display a very broad absorption band around of 822 cm^{-1}. These bands are assigned to $F_2(\nu_3)$ antisymmetric stretch vibrations, which were reported to be ascribed to the Mo–O stretching vibration in MoO_4^{2-} tetrahedra [21].

Figure 5 presents the room-temperature excitation spectra of $Sr_{1-x}Eu_xMoO_4$ (x=0.01; 0.03; 0.05) (SEMO) powders heat treated at 800 °C for 2 h, which were obtained setting the Eu^{3+} emission maximum at 614.6 nm. In these excitation spectra it was noticed the characteristic excitation band due to the $^5D_0 \rightarrow {}^7L_6$ transition of the $[EuO_8]^{\bullet}$ units observed at 394 nm and a broad band at 288 nm. The presence of this broad band is ascribed to charge transfer from the $[MoO_4]^{2-}$ ionic tetragonal clusters to the $[EuO_8]^{\bullet}$ ones. It is interesting to notice that the intensity of the broad band at around 288 nm presents almost the same value as the peak related to the $[EuO_8]^{\bullet}$ $^5D_0 \rightarrow {}^7L_6$ transition located at 394 nm. In the case of the $BaMoO_4$ doped with Eu^{3+} powders (BEMO), studied before by our group, the intensity of the energy transfer band is always smaller when compared to the intensity of the band related to the Eu^{3+} $^5D_0 \rightarrow {}^7L_6$ transition [22, 23]. It is worth to notice the enhancements of the characteristic emissions of these materials when this new route was used. The results show that the red phosphor was obtained mainly due to more efficiency in transferring charge transfer band

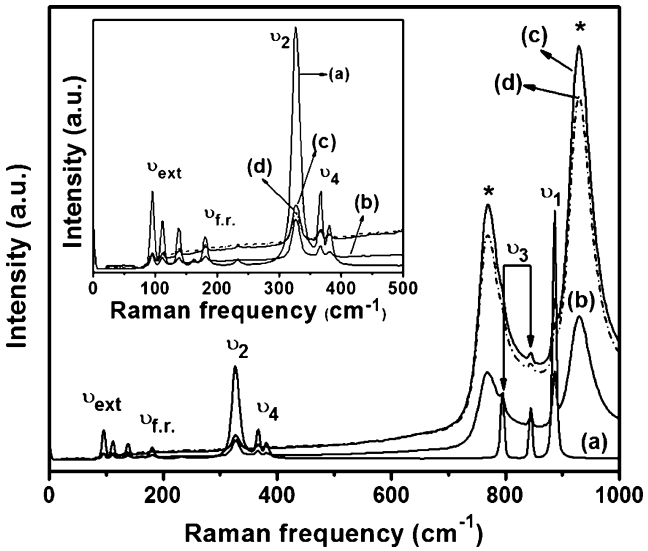

Fig. 3 Spontaneous Raman spectra of the SMO (a) and SEMO powders containing 1.00 (b), 3.00 (c) and 5.00% (d) of Eu^{3+} heat treated at 800 °C for 2 h

Table 2 Raman mode frequencies of SMO and SEMO powders prepared by CP Method

Lattice mode symmetry C_{4h}^6	SEMO[a]–Eu^{3+} %			SMO[b]	Assignments
	1.00	3.00	5.00		
A_g	929	929	928	886	ν_1 (A_1)
	886	886	886		
B_g	844	845	844	845	ν_3 (F_2)
E_g	793	793	794	795	
	772	770	771		
E_g	381	381	381	381	ν_4 (F_2)
B_g	367	367	367	367	
B_g	327	327	327	327	ν_2 (E)
A_g	232			234	
E_g	180	182	181	180	$\nu_{f.r.}$ (F_1) free rotation
B_g	161			163	$\nu_{ext.}$—external modes MoO_4^{2-} and Sr^{2+} motions
E_g	138	139	139	138	
B_g	112	112	112	112	
E_g	95	95	95	95	

[a] This present work

[b] Ref. [10]

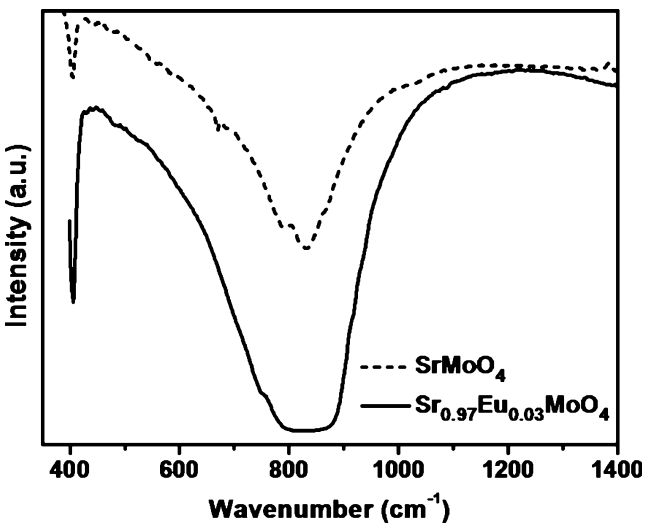

Fig. 4 FTIR absorption spectra of SMO and SEMO containing 3.00% of Eu^{3+}

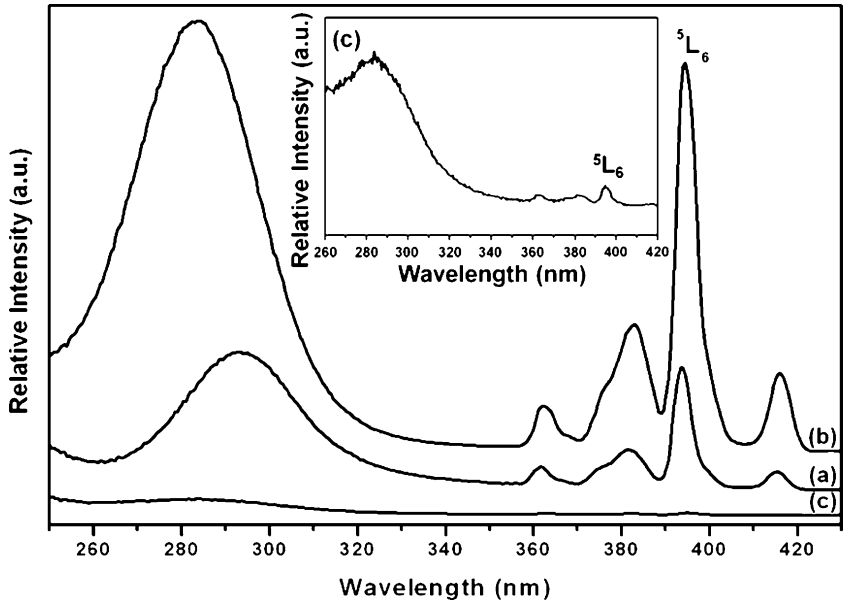

Fig. 5 Room-temperature excitation spectrum of $Sr_{1-x}Eu_xMoO_4$ powders, where x=0.01 (a), 0.03 (b), and 0.05 (c), heat treated at 800 °C for 2 h, when the emission is set at 614.6 nm. Inset: Zoom of excitation spectrum of $Sr_{0.97}Eu_{0.03}MoO_4$ powders

from $[MoO_4]^{2-}$ ionic tetragonal clusters to the $[EuO_8]^{\bullet}$ ones. This phenomenon reaches its maximum when the $[EuO_8]^{\bullet}$ clusters concentration is around 0.03 moles. Another advantage of this methodology in the synthesis of this material is the fact that the band length of the charge transfer band (from 260 to 320 nm, Fig. 5) makes possible the $[EuO_8]^{\bullet}$ clusters excitation in an ample range of the ultraviolet region of the spectrum. In this work it was also noticed that as the concentration increase the maximum wavelength shifts to higher wavelength. The maximum of this charge transfer band was observed at around 295 nm for the sample SEMO 1.00% of Eu^{3+}, while the samples SEMO 3.00% and 5.00% of Eu^{3+} presented the maximum

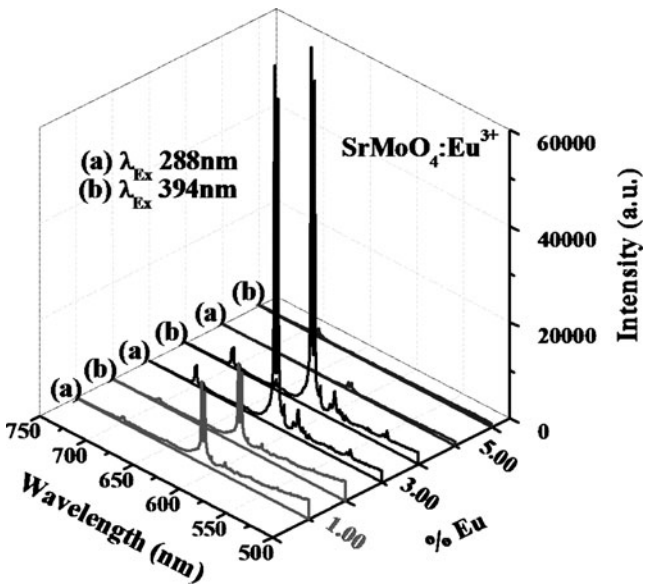

Fig. 6 Emission spectra of the $Sr_{1-x}Eu_xMoO_4$ (x=0.01; 0.03; 0.05) powders heat treated at 800 °C excited at 288 (a) and 394 nm (b)

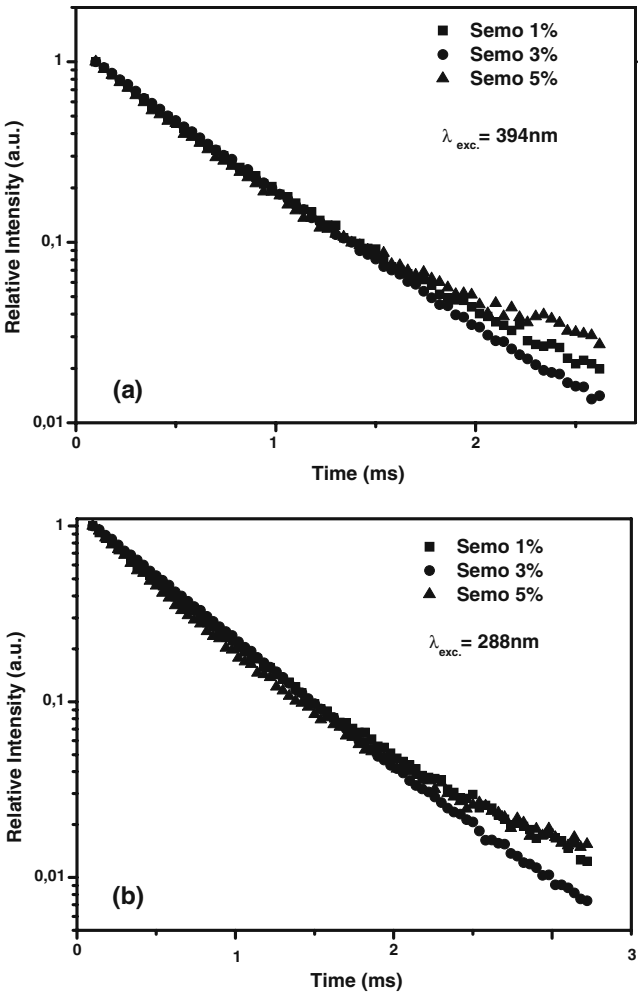

Fig. 7 Decay curves of the $^5D_0 \rightarrow {}^7F_2$ transition for the SEMO powder samples using the emission at 614.6 nm and excitation and 394 nm (**a**) and 288 nm (**b**)

Table 3 Eu^{3+} lifetime values (ms) of SEMO powders using the emission at 614.6 nm and excitation at 394 nm and 288 nm

Sample	Life time (ms) $\lambda_{EM.}$=614.6nm	
	$\lambda_{EXC.}$=394nm	$\lambda_{EXC.}$=288nm
SEMO 1.00% Eu^{3+}	0.53	0.57
SEMO 3.00% Eu^{3+}	0.54	0.60
SEMO 5.00% Eu^{3+}	0.49	0.51

at 288 nm. This charge transfer band is however reported in the literature with a maximum at 270 nm [18].

Figure 6 shows the emission spectra of the SEMO powders with different Eu^{3+} concentrations heat treated at 800 °C for 2 h, where the samples were excited at 288 and 394 nm. All samples presented the characteristic $[EuO_8]^{\bullet}$ clusters emission bands related to the $^5D_1 \rightarrow {}^7F_0$, $^5D_1 \rightarrow {}^7F_1$ and $^5D_1 \rightarrow {}^7F_2$ transitions at, respectively, 523, 533 and 554 nm, besides the $[EuO_8]^{\bullet}$ clusters $^5D_0 \rightarrow {}^7F_{0,1,2,3 \text{ and } 4}$ ones observed at around 578, 589, 614, 652 and 699 nm, respectively. The band referent to the $^5D_0 \rightarrow {}^7F_0$ transition indicates the presence of $[EuO_8]^{\bullet}$ clusters sites without inversion center. This hypothesis is strengthened by the fact that the band ascribed to the $^5D_0 \rightarrow {}^7F_2$ transition is the most intense in the emission spectra. It was observed through these spectra that the relative intensity of the Eu^{3+} emissions increase as the concentration of this ion increases from 0.01 to 0.03 mol. However, when the Eu^{3+} concentration is higher than this value the intensities of the emission bands are quenched drastically, as it is seen for the sample with 0.05 mol. This behavior indicates the presence of different energy transfer processes occurring in each situation. When the Eu^{3+} concentrations are smaller than 0.03 mol, the non-radiative mechanism of energy transfer between the Eu^{3+} ions is absent. It was observed however that the charge-transfer from the O 2p state ($[EuO_8]^{\bullet}$) to the Mo 4d state ($[MoO_4]^{2-}$) is present in this situation and increase as the Eu^{3+} concentration increases. The $[MoO_4]^{2-}$ ionic tetragonal clusters make an important role absorbing the excitation energy and transfer it then to the $[EuO_8]^{\bullet}$ ones. This process increases the population of the excited state of these clusters and promotes the enhancement of the emission. The increase in the intensity of the broad band is also ascribed to this phenomenon. Both of the described mechanisms contribute to the increase of the Eu^{3+} emission intensities. When the Eu^{3+} concentration is higher than 0.03 mol, however, the mechanism which prevails is the energy transfer from one $[EuO_8]^{\bullet}$ clusters to another. This energy migration process promotes an increase of the non-radiative relaxation, since the optical excitation is trapping at defects or impurity sites. In this way, the non-radiative transitions among different $[EuO_8]^{\bullet}$ clusters in the samples are responsible for the Eu^{3+} luminescence inhibition, the so called quenching concentration [23].

The decay curves of the $^5D_0 \rightarrow {}^7F_2$ transition for SEMO samples containing 1.00, 3.00, and 5.00% of Eu^{3+} were obtained using the emission at 614.6 nm and excitation at 394 or 288 nm. The decay curves followed a monoexponential behavior, as shown in the Fig. 7a and b. The life time values are also shown for each excitation wavelength applied in the Table 3.

The charge-transfer from the O (2p) state to the Mo (4d) one is present, and increase when Eu^{3+} concentration increases from 0.01 to 0.03 mol. The MoO_4^{2-} units absorb the excitation energy and then transfer it to the Eu^{3+}. This process presents slightly higher lifetime compared to the excitation at 394 nm.

References

1. Sczancoski JC, Cavalcante LS, Joya MR, Espinosa JWM, Pizani PS, Varela JA, Longo E (2009) Synthesis, growth process and photoluminescence properties of $SrWO_4$ powder. J Colloid Interface Sci 330:227–236
2. Cui C, Bi J, Gao D (2009) A simple chemical method for the deposition of highly crystallized $SrMoO_4$ films. J Alloys and Comp 470:21–24
3. Kiselev AP, Shmurak SZ, Red'kin BS, Sinitsyn VV, Shmyt'ko IM, Kudrenko EA, Ponyatovskii EG (2006) Evolution of the spectral response of amorphous europium molybdate under annealing. Phys Solid State 48(8):1544–1552
4. Canibano H, Boulon G, Palatella L, Guyot Y, Brenier A, Voda M, Balda R, Fernandez J (2003) Spectroscopic properties of new Yb^{3+}-doped $K_5Bi(MoO_4)_4$ crystals. J Lumin 102:318–326
5. Ma X, Li J, Zhu Z, You Z, Wang Y, Tu C (2008) Optical properties of Er^{3+}:$SrMoO_4$ single crystal. J Phys Chem Solids 69:2411–2415
6. Kubo J, Ueda W (2009) Catalytic behavior of $AMoO_x$ (A = Ba, Sr) in oxidation of 2-propanol. Mater Res Bull 44:906–912
7. Ma X, Zhu Z, Li J, You Z, Wang Y, Tu C (2009) Optical properties of Ho^{3+}:$SrMoO_4$ single crystal. Mater Res Bull 44:571–575
8. Rangappa D, Fujiwara T, Watanabe T, Yoshimura M (2008) Fabrication of $AMoO_4$ (A = Ba, Sr) film on Mo substrate by solution reaction assisted ball-rotation. Mater Res Bull 43:3155–3163
9. Mikhin SB, Mishin AN, Potapov AS, Rodnyi PA, Voloshinovskii AS (2002) X-ray excited luminescence of some molybdates. Nucl Instrum Methods Phys Res A 486:295–297
10. Marques APA, Melo DMA, Paskocimas CA, Pizani PS, Leite ER, Longo E (2007) Study of the photoluminescence $SrMoO_4$ powders synthesized by the complex polymerization method (CP METHOD). Ch 6. Nova Science, New York
11. Maurera MAMA, Souza AG, Soledade LEB, Pontes FM, Longo E, Leite ER, Varela JA (2004) Microstructural and optical characterization of $CaWO_4$ and $SrWO_4$ thin films prepared by a chemical solution method. Mater Lett 58:727–732
12. Marques APA, de Melo DMA, Paskocimas CA, Pizani PS, Joya MR, Leite ER, Longo E (2006) Photoluminescent $BaMoO_4$ nanopowders prepared by complex polymerization method (CP METHOD). J Solid State Chem 179:658–666
13. Rosa ILV, Oliveira LH, Suzuki CK, Varela JA, Leite ER, Longo E (2008) SiO_2-GeO_2 soot preform as a core for Eu_2O_3

nanocoating: synthesis and photophysical study. J Fluoresc 18 (2):541–545
14. Morais EA, Scalvi LVA, Tabata A, Oliveira JBB, Ribeiro SJL (2008) Photoluminescence of Eu^{3+} ion in SnO_2 obtained by sol–gel. J Mater Sci 43:345–349
15. Kodaira CA, Brito HF, Malta OL, Serra OA (2003) Luminescence and energy transfer of the europium (III) tungstate obtained via the Pechini method. J Lumin 101:11–21
16. Ma X, You Z, Zhu Z, Li J, Wu B, Wang Y, Tu C (2008) Thermal and optical properties of Tm^{3+}:SrMoO crystal. J Alloys Comp 465:406–411
17. Xu L, Zhiping Y, Li G, Qinglin G, Sufang H, Panlai L (2007) Synthesis and properties of Eu^{3+} activated strontium molybdate phosphor. J Rare Earths 25:706–709
18. Yang P, Li C, Wang W, Quan Z, Gai S, Lin J (2009) Uniform $AMoO_4$:Ln (A = Sr^{2+}, Ba^{2+}; Ln = Eu^{3+}, Tb^{3+}) submicron particles: solvothermal synthesis and luminescent properties. J Solid State Chem 182:2510–2520
19. JCPDS N°. 08-0482.
20. Basiev TT, Sobol AA, Voronko YK, Zverev PG (2000) Spontaneous Raman spectroscopy of tungstate and molybdate crystals for Raman lasers. Opt Mater 15(3):205–216
21. Nakamoto K (1986) Infrared and Raman spectra of inorganic and coordination compounds, 4th edn. Wiley, New York
22. Rosa ILV, Marques APA, Tanaka MTS, Melo DMA, Leite ER, Longo E, Varela JÁ (2008) Synthesis, characterization and photophysical properties of Eu^{3+} doped in $BaMoO_4$. J Fluoresc 18:239–245
23. Rosa ILV, Marques APA, Tanaka MTS, Motta FV, Varela JA, Leite ER, Longo E (2009) Europium(III) concentration effect on the spectroscopic and photoluminescent properties of $BaMoO_4$: Eu. J Fluoresc 19:495–500